

Alma Mater Studiorum Università di Bologna
Archivio istituzionale della ricerca

Capacity design of traditional and innovative ductile connections for earthquake-resistant CLT structures

This is the final peer-reviewed author's accepted manuscript (postprint) of the following publication:

Published Version:

Trutalli D., Marchi L., Scotta R., Pozza L. (2019). Capacity design of traditional and innovative ductile connections for earthquake-resistant CLT structures. BULLETIN OF EARTHQUAKE ENGINEERING, 17(4), 2115-2136 [10.1007/s10518-018-00536-6].

Availability:

This version is available at: <https://hdl.handle.net/11585/731047> since: 2020-02-22

Published:

DOI: <http://doi.org/10.1007/s10518-018-00536-6>

Terms of use:

Some rights reserved. The terms and conditions for the reuse of this version of the manuscript are specified in the publishing policy. For all terms of use and more information see the publisher's website.

This item was downloaded from IRIS Università di Bologna (<https://cris.unibo.it/>).
When citing, please refer to the published version.

(Article begins on next page)

This is the final peer-reviewed accepted manuscript of:

*Trutalli, D., Marchi, L., Scotta, R. et al. **Capacity design of traditional and innovative ductile connections for earthquake-resistant CLT structures.** Bull Earthquake Eng 17, 2115–2136 (2019)*

The final published version is available online at: <https://doi.org/10.1007/s10518-018-00536-6>

Rights / License:

The terms and conditions for the reuse of this version of the manuscript are specified in the publishing policy. For all terms of use and more information see the publisher's website.

This item was downloaded from IRIS Università di Bologna (<https://cris.unibo.it/>)

When citing, please refer to the published version.

Query Details

1. Please confirm the corresponding author is correctly identified and amend if necessary.

Corresponding author has been correctly identified

2. Please provide complete details for the reference Paulay and Priestley (1992).

John Wiley & Sons, Inc.

DOI:10.1002/9780470172841

Capacity design of traditional and innovative ductile connections for earthquake-resistant CLT structures

Davide Trutalli, ¹

Email davide.trutalli@dicea.unipd.it

Luca Marchi, ¹

Email luca.marchi@dicea.unipd.it

Roberto Scotta, ¹

Email roberto.scotta@dicea.unipd.it

Luca Pozza, ²✉

Email luca.pozza2@unibo.it

¹ Department of Civil, Environmental and Architectural Engineering, University of Padova, via Marzolo 9, 35131 Padua, Italy

² Department of Civil, Chemical, Environmental and Materials Engineering, University of Bologna, viale Risorgimento 2, 40136 Bologna, Italy

Received: 19 April 2018 / Accepted: 10 December 2018

Abstract

Traditional connections in earthquake-resistant cross-laminated timber buildings are susceptible of brittle failures, even when buildings are designed and supposed to be ductile. This is mainly due to the large underestimation of the actual strength of the ductile components, with consequent increased strength demand for the brittle parts, which may fail if designed with insufficient overstrength. Recent studies demonstrate that the use of steel connections characterized by a well-defined mechanical behaviour can improve significantly ductility and dissipative capacity of cross-laminated timber structures and the reliability of the capacity design. In this paper, the conceptual model of capacity design is discussed, proposing some modifications to improve its reliability for traditional and high-ductility connections for CLT structures. Results from quasi-static cyclic-loading tests of an innovative ductile bracket are presented and the corresponding overstrength factors are computed using the proposed conceptual method and compared with values available in the literature for traditional connections. Finally, a comparative application of the capacity criteria to the design of the innovative bracket and of a traditional nailed connection is presented and discussed.

AQ1

Keywords

Capacity design
CLT structures
Innovative connections
Overstrength factor
Timber structures

List of symbols

B	Brittle component (used as subscript)
D	Ductile component (used as subscript)
d_u	Ultimate displacement
d_y	Yielding displacement
$d_{y,est}$	Estimated yielding displacement
d_{peak}	Displacement corresponding to peak force
d_{target}	Target displacement for a ductile element
F_{code}^-	Characteristic load-bearing capacity estimated according to code
F_{peak}	Peak load-bearing capacity obtained by a test
F_{peak}^-	5th percentile of the peak load-bearing capacity obtained by tests

F_{peak}^{mean}	Mean value of the peak load-bearing capacity obtained by tests
F_{peak}^{+}	95th percentile of the peak load-bearing capacity obtained by tests
F_{target}	Force at target displacement obtained by a test
F_{target}^{-}	5th percentile of the force at target displacement obtained by tests
F_{target}^{mean}	Mean value of the force at target displacement obtained by tests
F_{target}^{+}	95th percentile of the force at target displacement obtained by tests
F_u	Ultimate or failure force obtained by a test
F^{1st}	Force measured in the first cycle at d_{target} from cyclic-loading tests
F^{3rd}	Force measured in the third cycle at d_{target} from cyclic-loading tests
F^M	Force measured at d_{target} from monotonic test
F_y	Yielding force obtained by a test
F_y^{-}	5th percentile of the yielding force obtained by tests
F_y^{mean}	Mean value of the yielding force obtained by tests
F_y^{+}	95th percentile of the yielding force obtained by tests
F_d	Design strength
F_d^{-}	Lower design load-bearing capacity
F_d^{+}	Upper design load-bearing capacity
$f_{ax,k}$	Characteristic withdrawal parameter of a fastener
$f_{h,k}$	Characteristic embedment strength of a fastener in the timber member
$M_{y,Rk}$	Characteristic yield moment of a fastener
k^{-}	5th percentile of a property obtained by tests
k^{mean}	Mean value of a property obtained by tests
k^{+}	95th percentile of a property obtained by tests
k_{el}	Elastic stiffness
k_{pl}	Post-elastic stiffness
β_{Sd}	Strength degradation between 1st and 3rd cycle at d_{target} , due to cyclic loading
γ_{cyc}	Strength degradation between monotonic and cyclic-loading curves at d_{target} or d_{peak}
γ_{an}	Analytical overstrength
γ_{sc}	Scattering of the target strength or scattering of the peak strength
γ_{Rd}	Overstrength factor
γ_m	Partial factor for material properties
γ_m^{-}	Partial factor for material properties in calculating lower design value of the load-bearing capacity according to code

γ_m^+	Partial factor for material properties in calculating upper design value of the target force or the peak force
ρ_k	Characteristic value of wood density
μ	Ductility
ν_{eq}	Equivalent viscous damping

1. Introduction

The seismic response of cross-laminated timber (CLT) structures is strictly correlated to ductility and energy dissipation capacity of connections, which can be exploited only if they are designed according to reliable capacity-design rules.

Typical connections used in CLT structures are specifically optimized and manufactured to prevent the horizontal sliding or vertical uplift of the wall panels. These elements, known respectively as angle brackets and hold-downs, are hereafter identified as traditional connections. They are normally made of punched and cold-formed thin steel plates fastened to the panel generally with ring shank nails or screws. Ductility and energy dissipation capacities of traditional connections rely entirely on cyclic behaviour of the dowel-type fasteners, whereas the steel plates and all the timber members should be over-resistant to prevent premature brittle failures. Wood embedment of fasteners (i.e., nails or screws) leads to a marked pinching behaviour of steel-to-timber connections, limiting their dissipative capacity and therefore the seismic performance of the entire CLT structure, especially if realized with unfavourable geometrical configuration and panel arrangement (Pozza and Trutalli 2017).

Actually, traditional connections are the same that were originally developed for light-frame shear walls, with some geometrical improvements to assure higher load-bearing capacities [e.g., (Tomasi and Smith 2015; Polastri and Pozza 2016; Izzi et al. 2018a)]. However, in light-frame technology energy dissipation capacity is assured by small-diameter fasteners (e.g., screws or nails), that diffusively connect bracing panels to the light frame, allowing shear deformation of walls. On the contrary, CLT panels are elastic and almost infinitely rigid in their plane, therefore energy dissipation is localized only into reciprocal connections between panels and to the ground.

A possible strategy to improve the ductility and the seismic response of CLT buildings with traditional connections is the fragmentation of the façades into narrow modular panels, vertically jointed by means of small-diameter screws or nails. This improvement has been quantified by analysing full-scale tests of CLT

shear walls (Pozza et al. 2016), via parametric numerical analyses (Pozza and Trutalli 2017; Izzi et al. 2018b) and by comparison of shake-table tests of different buildings (Ceccotti 2008; Flatscher and Schickhofer 2015). However, fragmentation of panel is in contrast with advantages of prefabricated systems, i.e., ease and speed of assembling.

A more affordable strategy is based on the adoption of connection elements with optimized cyclic behaviour to guarantee a high level of ductility and dissipative capacity to CLT buildings, independently of the organization and dimension of CLT panels. These devices are hereafter called innovative connections. The use of special steel devices as dissipative connections has been widely investigated (Kelly et al. 1972) and found application in the design of connections for reinforced concrete (RC) structures (Henry et al. 2010). More recently, various types of innovative connection for CLT buildings have been developed, which exploit the hysteretic behaviour of steel (Baird et al. 2014; Latour and Rizzano 2015; Scotta et al. 2016; Schmidt and Blaß 2017; Polastri et al. 2017) or friction (Loo et al. 2014; Hashemi et al. 2017). These connections work in an opposite way with respect to traditional connections: the deformation is localized in the dissipative component, whereas the anchoring to the CLT panel must guarantee negligible elastic deformations, resulting in a limited pinching effect and a better control of the seismic response of the entire connection and, therefore, of the entire building.

In summary, independently from the adopted construction method (continuous horizontal panels, or narrow modular panels) and from the chosen type of connection (traditional or innovative), the optimal design of an earthquake-resistant CLT building should comply with a rigorous capacity-design approach to avoid brittle failures and ensuring maximum ductility and dissipative capacity to shear-wall systems (Jorissen and Fragiaco 2011). The compliance of the seismic design of CLT structures with this approach is even more important than in designing RC and steel structures, for which most regions outside the defined non-linear zones still possess non-linear capacity (Smith et al. 2015).

The aim of this work is to propose some conceptual modifications to the model of capacity design to make it better adaptable to traditional and innovative connections for CLT panels and to improve its reliability, starting from the necessary literature background. Results from the latest experimental tests of an innovative high-ductility device are presented and exploited to examine the practical suitability of the modified conceptual model. This connection element is a tension-shear resistant steel bracket, which can highly improve ductility and energy dissipation capacity of CLT buildings. The statistical distribution of the main mechanical parameters obtained from tests of the bracket is here presented

and analysed to estimate the overstrength factors, in comparison with values for traditional connections provided by the literature. Finally, the conceptual model of capacity design is analytically applied to the fastening to the CLT panel of the tested bracket, validated through an additional experimental test, and to the fastening to the CLT panel of a traditional hold-down, according to experimental values available in the literature.

2. Overview on capacity design of connections in CLT buildings

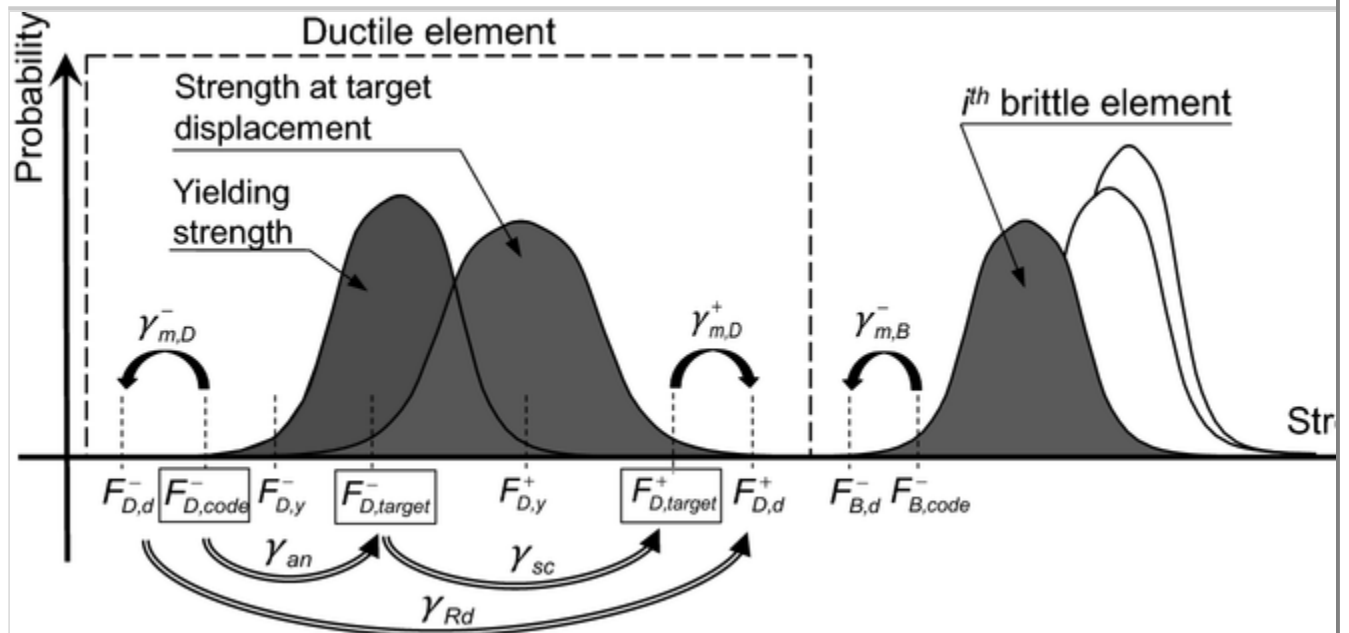
In this section, a modified conceptual model of capacity design and the main literature background are presented, with the aim of discussing the definition of overstrength factor and its application to design the brittle components of a connection, starting from the evaluation of the strength properties of its ductile part. In the following approach, the component of the connection system which is desirable to deform plastically is identified as ductile, whereas all the other components, which are brittle or less ductile, are in any case identified as brittle. For example, considering a connection for CLT structures and according to what was discussed in the Introduction, if capacity design is to be applied to a traditional connection, fasteners are considered the ductile part of the system; on the contrary, if capacity design is to be applied to an innovative connection, fasteners that anchor the device to the panel are considered the brittle part of the system, even if they have an elastoplastic behaviour.

2.1. Conceptual model of capacity design

The capacity design approach was originally developed for RC structures (Paulay and Priestley 1992). Its extension to timber and even to CLT structures has been already formally defined and is available in the literature (Fragiacomo et al. 2011; Jorissen and Fragiaco 2011; Gavric et al. 2013). Figure 1 shows a modified conceptual model, starting from the model in Jorissen and Fragiaco (2011), of the capacity design of the brittle components of the system (subscript B), depending on the statistical distribution of the strength of the ductile part (subscript D) and the analytical procedures and factors applied by practitioners to evaluate such strength (i.e., rules and factors according to codes or standards). The model presented here aims to give a comprehensive approach of capacity design and to introduce some concepts:

Fig. 1

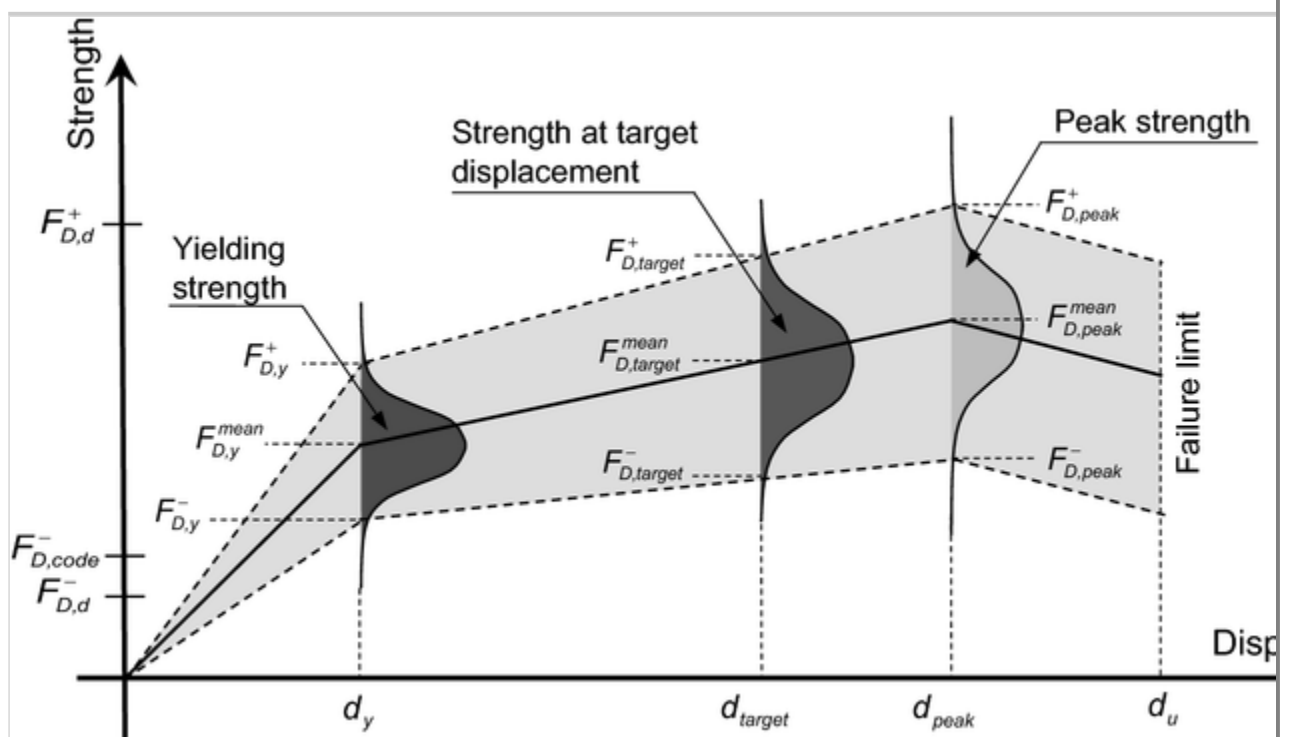
Conceptual model of capacity design applied to a ductile component with $d_{target} < d_{peak}$ (for cases with $d_{target} \geq d_{peak}$, the subscript “target” has to be changed with “peak”)



1. Since a ductile element could reach very high displacements, a proper target displacement d_{target} is defined as limit of the displacement capacity according to the seismic performance demand, Fig. 2. It is necessary to assure that the ductile element of the structure be able to deform up to d_{target} , avoiding not only the failure of the brittle components but also their possible incompatible deformations, which could compromise the effectiveness of the ductile element.

Fig. 2

Yielding, target and peak strength of a ductile element and their statistical distribution. $d_{target} < d_{peak}$



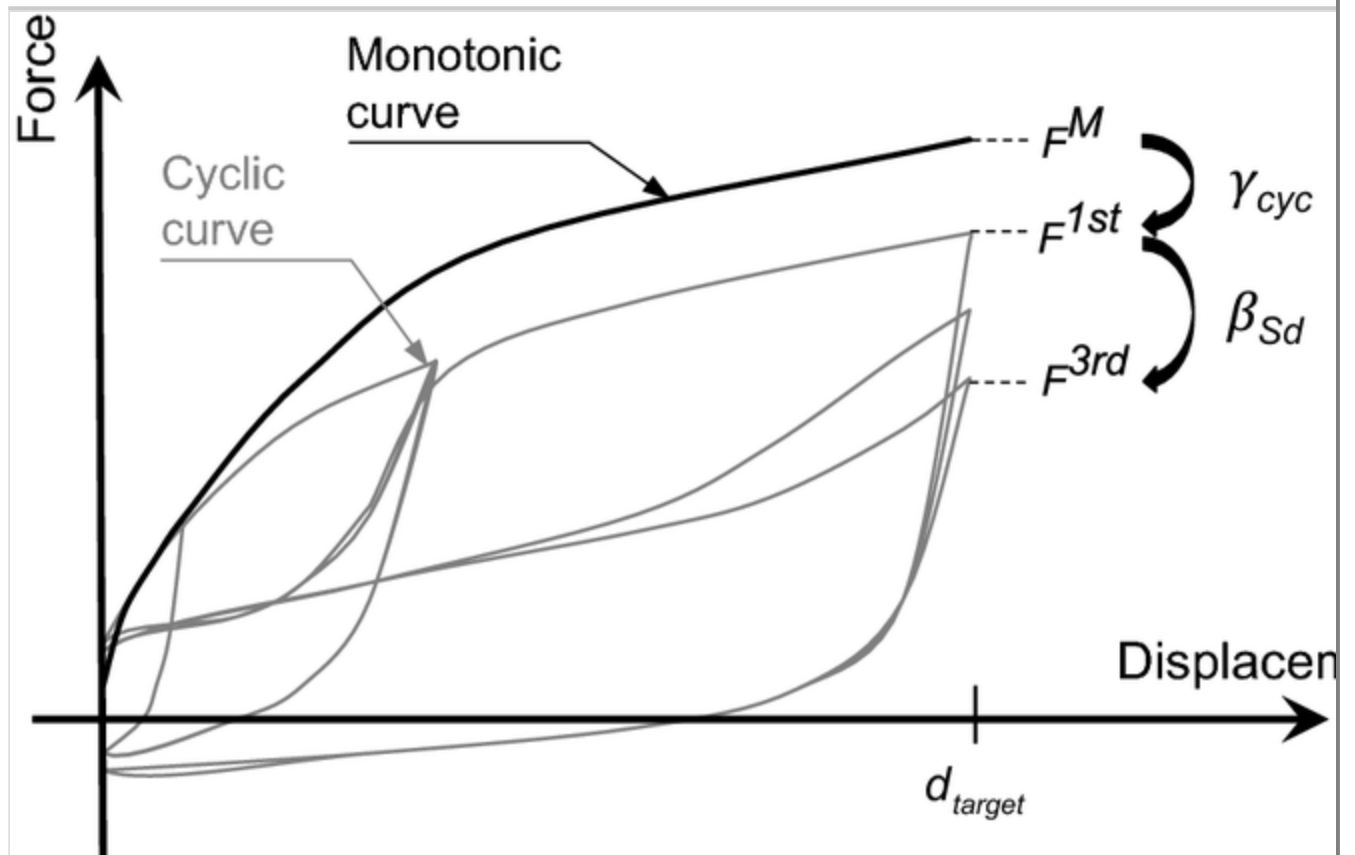
2. The partial factor for material properties γ_m has been introduced in the capacity design model also in the amplification of the strength of the ductile component to obtain the upper design value. The possibility of having a different γ_m depending on its application in calculating the lower or the upper design value of a strength property is also considered.

Figure 1 shows two groups of curves, which schematize a statistical distribution of the strength of all the structural components of a connection system. The two curves on the left identify the ductile component, whose strength must be compared with that of the weakest brittle component (*i*th brittle element of the curves on the right). According to Fig. 2, $F_{D,y}^-$, $F_{D,y}^{mean}$ and $F_{D,y}^+$ are the 5th percentile, mean value and 95th percentile of the yielding strength of the ductile element obtained by tests; $F_{D,target}^-$, $F_{D,target}^{mean}$ and $F_{D,target}^+$ refer to the strength corresponding to d_{target} ; $F_{D,peak}^-$, $F_{D,peak}^{mean}$, and $F_{D,peak}^+$ refer to the peak strength. The actual failure load F_u , as defined according to standards for loading tests [e.g., EN 12512 (CEN 2005)], is normally different from the maximum strength F_{peak} , admitting an amount of softening deformation after the peak force, reaching an ultimate displacement d_u higher than the displacement at maximum strength d_{peak} . The displacement d_{target} can be therefore lower or higher than d_{peak} but always lower than or equal to d_u .

It is worth noting that the parameters listed above should be obtained with monotonic tests, because normally the envelope curve obtained in cyclic loading may be affected by strength degradation, resulting in a not conservative capacity design, Fig. 3. In this case, the different strength between the first cyclic envelope (F^{1st}) and the monotonic curve (F^M) should be considered by means of a specific factor γ_{cyc} in the capacity design, to increase the strength obtained with cyclic-loading tests.

Fig. 3

Definition of strength degradations in cyclic loading



Based on the definitions set out above, the capacity design consists in fulfilling inequality (1), i.e., the lower design value of the characteristic load-bearing capacity of the brittle parts of the system estimated according to code $F_{B,d}^-$ must be higher or equal to the upper design value $F_{D,d}^+$ of the maximum 95th percentile strength reached by the ductile element up to d_{target} . In this way, the ductile element is able to reach d_{target} without exceeding $F_{B,code}^-$ with a fixed probability according to ultimate-limit-state (ULS) approach (CEN 2010). Two hypotheses are therefore possible:

1. $d_{target} < d_{peak}$. In this case the target displacement is within the hardening behaviour before the peak strength. $F_{D,d}^+$ is defined as product between $F_{D,target}^+$ and the partial factor for material properties $\gamma_{m,D}^+$.
2. $d_{target} \geq d_{peak}$. In this case, the 95th percentile of the force at d_{target} , i.e., $F_{D,target}^+$, is normally lower than the 95th percentile of the peak strength $F_{D,peak}^+$. $F_{D,d}^+$ is defined as product between $F_{D,peak}^+$ and the partial factor for material properties $\gamma_{m,D}^+$.

$$\frac{F_{B,code}^-}{\gamma_{m,B}^-} = F_{B,d}^- \geq F_{D,d}^+ = \begin{cases} F_{D,target}^+ \cdot \gamma_{m,D}^+, & d_{target} < d_{peak} \\ F_{D,peak}^+ \cdot \gamma_{m,D}^+, & d_{target} \geq d_{peak} \end{cases} \quad 1$$

The overstrength factor γ_{Rd} is introduced to have a direct comparison between the lower design load-bearing capacity of both ductile and brittle part ($F_{D,d}^+$, $F_{B,d}^-$), which are the only calculable values by practitioners. The capacity design is therefore code dependent because γ_{Rd} is strictly correlated to the analytical methods and the parameters used to compute the load-bearing capacity of the ductile element according to a particular code or design method, $F_{D,code}^-$. γ_{Rd} can be therefore defined as ratio between $F_{D,d}^+$ and $F_{D,d}^-$, Eq. (2).

$$\gamma_{Rd} = \frac{F_{D,d}^+}{F_{D,d}^-} = \begin{cases} \frac{F_{D,target}^+ \cdot \gamma_{m,D}^+}{F_{D,code}^- / \gamma_{m,D}^-} = \frac{F_{D,target}^+}{F_{D,code}^-} \cdot \gamma_{m,D}^+ \cdot \gamma_{m,D}^-, & d_{target} < d_{peak} \\ \frac{F_{D,peak}^+ \cdot \gamma_{m,D}^+}{F_{D,code}^- / \gamma_{m,D}^-} = \frac{F_{D,peak}^+}{F_{D,code}^-} \cdot \gamma_{m,D}^+ \cdot \gamma_{m,D}^-, & d_{target} \geq d_{peak} \end{cases} \quad 2$$

According to this definition, the overstrength factor γ_{Rd} includes two partial factors for material properties and two components of overstrength. The first overstrength sub-factor is the analytical overstrength γ_{an} , depending on the underestimation of the actual strength using the load-bearing capacity according to a particular code, Eq. (3); the second overstrength sub-factor is the experimental scattering γ_{sc} of the peak or target strength, Eq. (4).

$$\gamma_{an} = \begin{cases} F_{D,target}^- / F_{D,code}^-, & d_{target} < d_{peak} \\ F_{D,peak}^- / F_{D,code}^-, & d_{target} \geq d_{peak} \end{cases} \quad 3$$

$$\gamma_{sc} = \begin{cases} F_{D,target}^+ / F_{D,target}^-, & d_{target} < d_{peak} \\ F_{D,peak}^+ / F_{D,peak}^-, & d_{target} \geq d_{peak} \end{cases} \quad 4$$

Inequality (1) can be rewritten according to definition of γ_{Rd} in Eq. (2) or definitions of γ_{an} and γ_{sc} in Eqs. (3)–(4), obtaining the actual definition of capacity design, Eq. (5).

$$F_{B,d}^- \geq F_{D,d}^+ = \gamma_{Rd} \cdot F_{D,d}^- = \gamma_{an} \cdot \gamma_{sc} \cdot \gamma_{m,D}^+ \cdot \gamma_{m,D}^- \cdot F_{D,d}^- \quad 5$$

This formulation is of general validity. Specifically, the introduction of the partial factor for material properties, to be multiplied twice by $F_{D,d}^-$ in the capacity design, is new in the literature. The explanation can be given considering that, as γ_m should divide the 5th percentile of strength to obtain the lower design value, the same should be made to obtain the upper design value, multiplying the 95th percentile of strength by γ_m . The probabilistic approach of

the limit-state design makes also possible that γ_m^+ and γ_m^- be different. An important simplification can be made, considering that in the seismic design, all the partial factors for material properties in the previous Equations, both for the ductile and the brittle parts, can be taken equal to 1.0, accepting a higher probability of failure during an Earthquake (CEN 2013). In this case, Eq. (5) can be rewritten as in Eq. (6) to apply the capacity design directly to the characteristic load-bearing capacities according to codes or standards.

$$F_{B,code}^- \geq \gamma_{Rd} \cdot F_{D,code}^- \quad 6$$

Even if the concepts reported above are of general validity, when the ductile components are connectors for timber members additional notes are worth considering. According to the proposal in Follesa et al. (2015, 2018), Izzi et al. (2016), an additional term should be included in the previous equations of capacity design, because it has been introduced in the evaluation of the design strength of the ductile component: the factor β_{Sd} , (defined as ratio between force obtained at 3rd and 1st cycle, F^{3rd}/F^{1st}) accounting for the strength degradation due to cyclic loading (Fig. 3). In particular, factor β_{Sd} (≤ 1.0) should multiply $F_{D,code}^-$ in the calculation of $F_{D,d}^-$ for ULS verifications, in order to obtain the load-bearing capacity of the third loading cycle. For this reason, in the application of capacity design, $F_{D,d}^-$ has to be divided by β_{Sd} in order to come back, correctly, to the first-cycle strength. However, in the seismic design of connections, the cyclic strength reduction is already considered in the definition of the behaviour q-factor, according to Eurocode 8 (CEN 2013), used to compute the design forces in the ductile components. For this reason, it seems not necessary to introduce factor β_{Sd} in the calculation of the design strength, and, as a consequence, it does not appear in the model of capacity design proposed here.

2.2. Background literature on capacity design of CLT structures according to Eurocodes

Eurocode 8 (CEN 2013) currently provides overstrength factors γ_{Rd} for steel and RC structures only (in the range 1.0–1.3), whereas no specific provisions are given for timber structures (Fragiacomo et al. 2011). Therefore, there is the need to provide reliable overstrength factors also for CLT structures, which should be specific for each ductile element, i.e., dowel-type fasteners for traditional connections or steel brackets for innovative connections. A proposal for revision of Chapter 8 of Eurocode 8 (CEN 2013) is available in the literature (Follesa et al. 2015, 2018) where a γ_{Rd} equal to 1.3 for the CLT building technology and the formulations for its application in the capacity design are proposed.

The main issue in applying capacity design to traditional connections derives from the uncertainty in evaluating the actual peak strength of fasteners (i.e., the ductile component), which often largely exceeds the corresponding characteristic load-bearing capacity, $\overline{F_{D,code}^-}$, evaluated according to Johansen's Theory (Johansen 1949). Moreover, $\overline{F_{D,code}^-}$ is currently not univocally defined depending on the chosen values of parameters in the calculation model, according to the applied code, e.g., Eurocode 5 (CEN 2009), or special rules provided by product approvals (ETA). It is worth noting that, employing CLT instead of glulam or solid wood, the uncertainty in the analytical model to compute $\overline{F_{D,code}^-}$ of a fastener may increase. The direct consequence of such evidences and of the high standard deviation values normally exhibited by the ductile part of traditional connections is that the actual peak strength of fasteners might exceed the maximum strength of brittle components, with subsequent brittle failure of the entire connection. Therefore, the reliability of $\overline{\gamma_{Rd}}$ is affected by the statistical variability of the strength of the ductile element (high $\overline{\gamma_{sc}}$ are expected) and by the analytical method to estimate its characteristic strength, according to a particular code (high $\overline{\gamma_{an}}$ are expected). It is therefore of crucial relevance that the $\overline{\gamma_{Rd}}$ values proposed by a code be consistent with the analytical method and parameters suggested by the same code.

Some research studies in the literature deal with capacity design for CLT structures with traditional connections (Fragiacomo et al. 2011; Sustersic et al. 2012; Gavric et al. 2015a, b; Izzi et al. 2016; Ottenhaus et al. 2017). The statistical distribution of peak strength and the correspondent overstrength factors can be found in some research works. Izzi et al. (2016) conducted an exhaustive research about steel-to-timber joints with ring shank nails, deriving overstrength factors suitable for applying the capacity design to metal connections, as hold-downs and angle brackets; Ottenhaus et al. (2017) presented an evaluation of overstrength factor for dowelled connections; Gavric et al. (2015a) analysed the behaviour of typical angle brackets and hold-downs and of typical screwed connections. The resulting $\overline{\gamma_{Rd}}$ for steel-timber connections with ring shank nails are in the range 1.6–2.6 (Izzi et al. 2016), depending on the calculation of $\overline{F_{D,code}^-}$ and on the angle of the shear force to the face lamination of the panel, thus demonstrating the strict correlation between $\overline{\gamma_{Rd}}$ and the analytical model to compute $\overline{F_{D,code}^-}$. For typical angle brackets and hold-downs $\overline{\gamma_{sc}}$ are given in Gavric et al. (2015a) in the range 1.16–1.44. The determination of $\overline{F_{D,code}^-}$ according to Eurocode 5 (CEN 2009), available in the same work, makes possible also the extrapolation of $\overline{\gamma_{Rd}}$, obtaining values in the range 2.0–3.4. According to Ottenhaus et al. (2017), $\overline{\gamma_{Rd}}$ for steel-to-timber connections with dowels was theoretically estimated to be equal to 1.68,

splitting this factor within different sources of overstrength; experimental tests were also performed to verify such estimation. Finally, in Gavric et al. (2015b) results from an extensive experimental programme of screwed connections returned values of γ_{sc} in the range 1.22–1.95 considering only specimens showing a ductile failure. Also in this case, γ_{Rd} can be extrapolated from $F_{D,code}^-$ according to Eurocode 5 (CEN 2009), resulting in a range 1.2–2.1. The main evidence from such estimations is the variability of γ_{Rd} for connections in CLT structure, reaching also values close to 3.0.

As concerning innovative connections, which employ the hysteretic behaviour of steel, keeping elastic the anchoring to the panel, no rules are normally available to evaluate analytically their load-bearing capacity and no works are available in the literature, which characterize these connections in terms of application of capacity design. The recognized rule applicable to steel elements, consisting in taking $F_{D,code}^- = F_{D,y}^-$ (CEN 2015) can be extended to these types of connection. It is worth noting that when strength and stiffness of the connection are governed only by steel property and geometry of the device, $F_{D,y}^-$ might be computed also by means of detailed finite-element analyses with two- or three-dimensional elements, thanks to the good accuracy in predicting the behaviour of steel and the yielding point. In this case, a suitable curve fitting the elastoplastic behaviour of steel [e.g., the Ramberg–Osgood law (Ramberg and Osgood 1943)] may be used according to tests of specimens of the selected steel. It seems therefore appropriate to state that employing connections with a well-defined yielding point and predictable target and peak strength results in a more reliable application of the capacity design. Therefore, research studies to characterize innovative high-ductility connections also in terms of correct application of capacity design are needed.

3. Evaluation of overstrength for a high-ductility connection

The actual applicability to innovative connections for CLT structures of the conceptual model of capacity design presented in the previous sections is verified through the study of a high-ductility connection. Results from tests of the ductile element are firstly analysed to define its cyclic behaviour and the overstrength factors. Then, a final test of the complete connection, composed by the ductile and brittle components, designed in accordance with capacity design, is presented to validate the model. This section presents also the final version of the connection and the experimental data for its mechanical characterization.

3.1. Experimental characterization

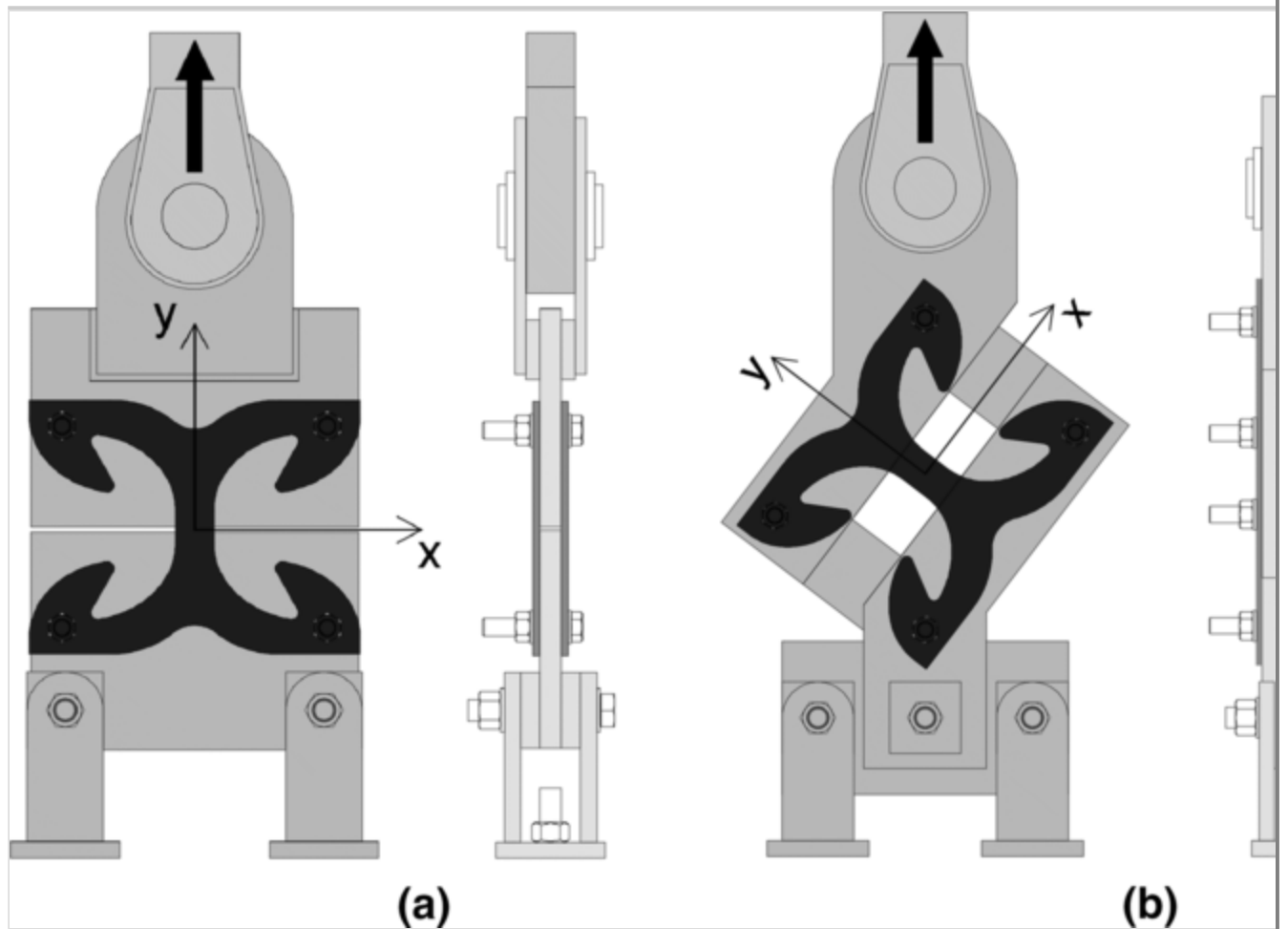
3.1.1. Description of the bracket and test setup

An innovative steel bracket has been developed at the University of Padova, as an alternative to traditional connections, to improve ductility and dissipative capacity of CLT buildings, and to have a better control of the seismic response, thanks to a well-defined mechanical behaviour. This connector is made by a single cutting of a steel plate, resulting in several X-shape brackets with four fixing points (16-mm diameter holes) necessary for the anchoring to the timber panel or to the foundation. Henceforth, this connection is called *X-bracket*. Detailed information about the design of the first prototype is available in Scotta et al. (2016) and its coupled shear/tension behaviour is described in Marchi et al. (2016). The final version of the bracket, here presented, has been obtained applying shape adjustments to the first prototype, with the aim to improve ductility and dissipative capacity. A 6-mm thick steel plate, with strength corresponding to a S450 steel grade according to EN 10025-2 (CEN 2004), was chosen to realize the latest specimens, cyclically tested in the mechanical laboratory of Department ICEA of the University of Padova. The effects of changes in thickness or steel grade, that obviously modify the yielding and ultimate strength of the bracket, could be evaluated through preliminary FE models. However, the expected slight differences in the cyclic behaviour and buckling are to be verified with additional experimental tests.

Six mechanical tests (three in tension and three in shear) were performed according to the quasi-static cyclic-loading protocol of EN 12512 (CEN 2005), imposing a yielding displacement $d_{y,est}$ equal to 4 mm. The same test procedure presented in Scotta et al. (2016) was followed, anchoring a couple of *X-brackets* to a rigid steel frame, with M16 8.8-class steel bolts (Fig. 4). Therefore, six brackets were tested in tension and six in shear. The shear test was performed using an unbraced steel truss, in which the *X-brackets* worked as cross-bracing elements (see Fig. 4b) positioning the specimens in a rotated configuration, in order to keep the loading direction as close as possible to the virtual diagonal line.

Fig. 4

Test setup of the innovative bracket: **a** tests in tension; **b** tests in shear

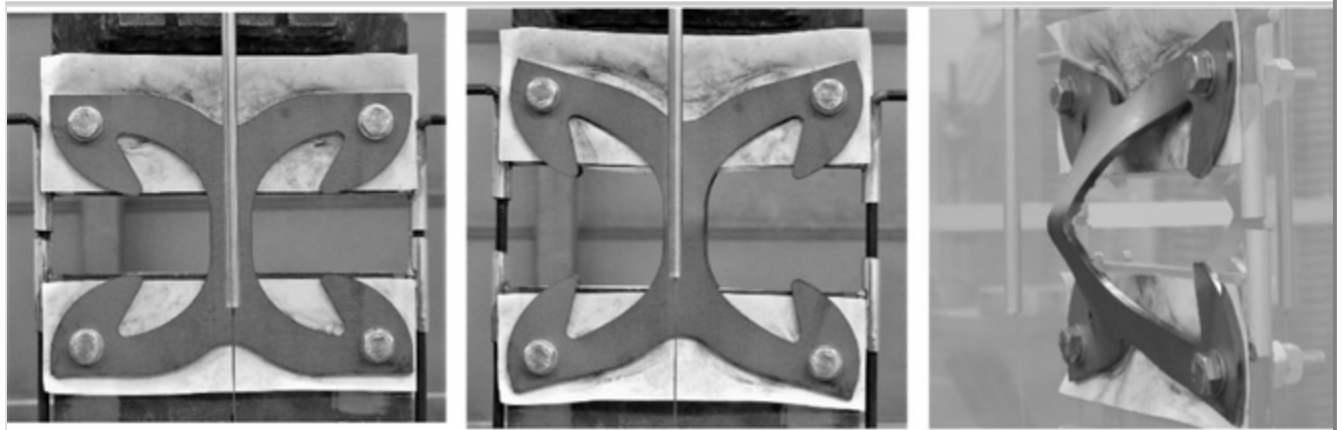


3.1.2. Test results

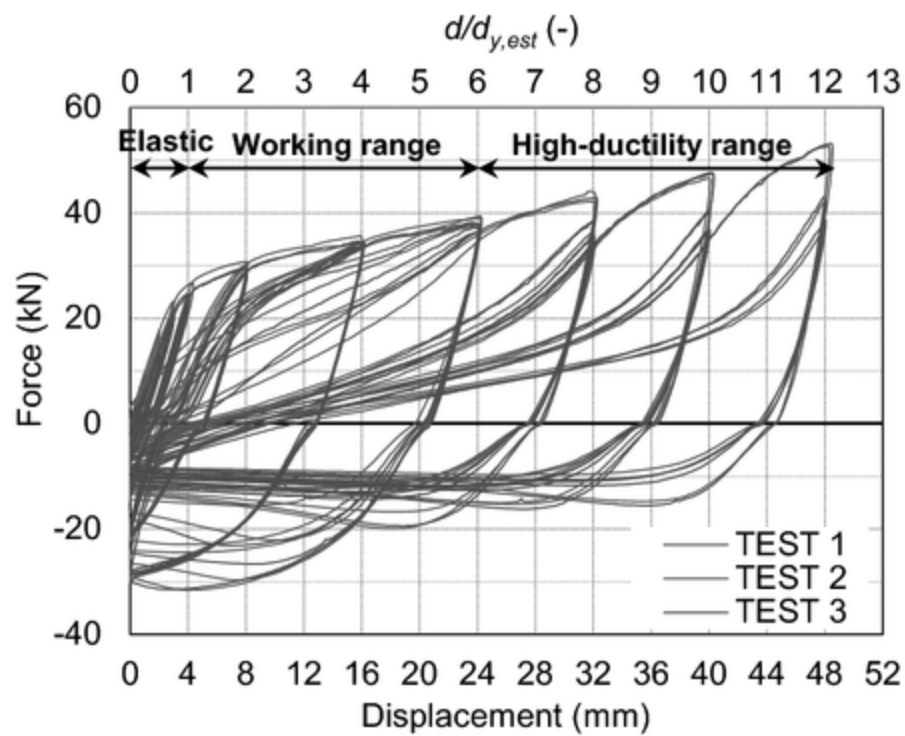
Test results are plotted in Figs. 5 and 6 in terms of force–displacement curve for all the tests. Strength refers to a single *X-bracket* device. With reference to the curves of the specimens loaded in shear (Fig. 6b), the projection of forces and displacements to the local axis x (see Fig. 4b) are shown, to present the results in terms of lateral force and lateral displacements of the bracket.

Fig. 5

Tension tests of the *X-bracket*: **a** undeformed specimen, specimen at d_{target_2} (40 mm), residual deformation after three cycles at d_{target_2} ; **b** force–displacement curves for a single bracket ($d_{y,est} = 4.00$ mm)



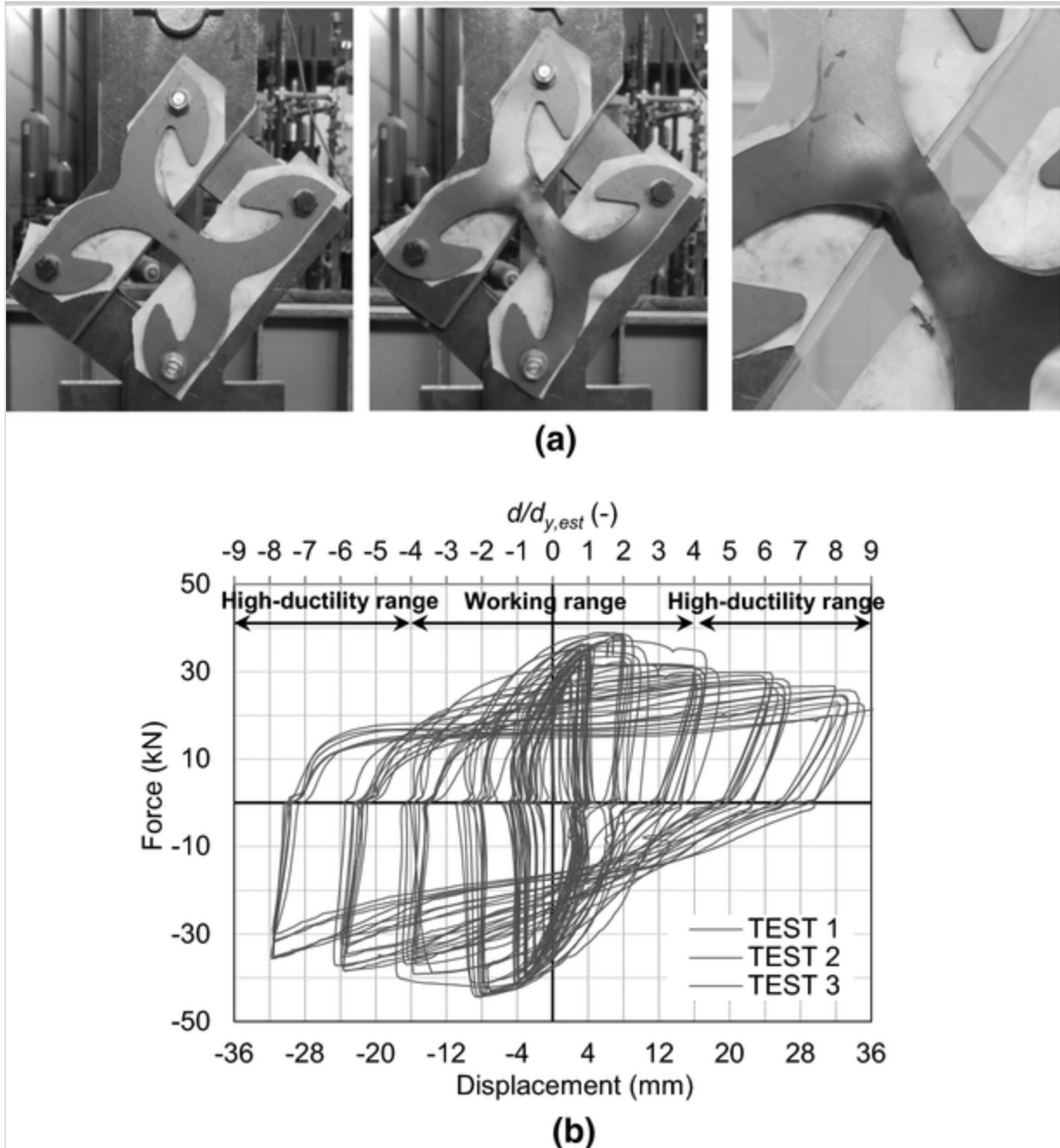
(a)



(b)

Fig. 6

Shear tests of the *X-bracket*: **a** undeformed specimen, specimen at d_{target} (24 mm), accumulation of plastic strain at d_{target} ; **b** force–displacement curves for a single bracket ($d_{y,est} = 4.00$ mm)



In tension tests, a homogeneous diffusion of yielding area between web and flanges gave to the bracket a great displacement capacity, and consequent high ductility and dissipated energy. Failure occurred for large displacements, due to out-of-plane flexural buckling of the vertical web during the unloading phase and consequent strength degradation in tension and compression (Fig. 5). Buckling and strength degradation were activated for a displacement of 24 mm, whereas for smaller displacements full hysteresis cycles were recorded and, therefore, maximum dissipation is assured. Despite this buckling phenomenon, a good hysteretic response was observed also for larger displacements, completing all the three repeated cycles also for the subsequent amplitudes (Fig. 5b), assuring in this way a very high ductility. Two target displacements, $d_{target_1} =$

24 mm and $d_{target_2} = 40$ mm, corresponding to $6d_{y,est}$ and $10d_{y,est}$ respectively, were assumed for all three tests.

Also for shear tests, failure was localized in the vertical web subjected to lateral torsional buckling (Fig. 6a), which started for large deformations (± 16 mm cycles in Fig. 6b). The failure mode can be explained by the inversion of loading, which led to an accumulation of large plastic strains in a relatively small area. However, all the three ± 24 mm cycles were completed without showing excessive strength degradation (Fig. 6b). This displacement was assumed as target displacement $d_{target} = 24$ mm.

From the hysteresis curves of the bracket in tension and shear (Figs. 5b and 6b) at force equal to zero (i.e., at the intersection of curves with x-axis), it is possible to observe the effects of small gap at the dowelled joint between the steel frame and the hydraulic jack. This gap caused a sudden disturbance, during the inversion of load, which was transmitted to the steel frame and captured by the linear variable displacement transducers.

The performed cyclic-loading tests allowed to define the main mechanical parameters and the statistical distribution of strength and stiffness. Table 1 lists elastic and post-elastic stiffness (k_{el} , k_{pl}), yielding point (d_y , $F_{D,y}$), peak and/or target point (d_{peak} , $F_{D,peak}$), (d_{target} , $F_{D,target}$), ductility μ . Yielding point and stiffness were obtained fitting the envelope of the hysteresis curves using the analytical formulation proposed by Foschi and Bonac (Foschi and Bonac 1977) and applying proper bi-linearization methods. In particular, due to the different post-elastic behaviour of the connector subjected to tension or shear, method (a) of EN 12512 (CEN 2005) was chosen for tests in tension, whereas the equivalent energy elastic–plastic (EEEP) method (Foliente 1996) was considered more suitable for the shear tests. From the obtained bi-linear curves, it was possible to classify the proposed connection into the suitable ductility class [Low (L), Medium (M) and High (H)], according to Eurocode 8 (CEN 2013). The 5th percentile and the 95th percentile (k^- , k^+) of the strength and stiffness parameters were calculated assuming a normal distribution according to EN 1990 (CEN 2010) and EN 14358 (CEN 2006).

Table 1

Main mechanical parameters according to EN 12512 method “a” (CEN 2005) for tensio method (Foliente 1996) for shear tests

Test	Parameter (units)	TEST 1	TEST 2	TEST 3	k^{mean}	SD	COV	EN 1990	
								k^-	k^+
In bold the values used to compute γ_{Rd}									

Test	Parameter (units)	TEST 1	TEST 2	TEST 3	k^{mean}	SD	COV	EN 1990	
								k^-	k^+
Tension tests	$F_{D,y}$ (kN)	28.59	29.51	28.16	28.75	0.62	2.14%	27.41	30.09
	d_y (mm)	3.26	3.08	3.21	3.18	0.08	2.53%	3.01	3.36
	$F_{D,target_1}$ (kN)	37.79	38.98	38.00	38.26	0.57	1.48%	37.02	39.50
	d_{target_1} (mm)	24.00	24.00	24.00	24.00	—	—	—	—
	μ (d_{target_1}) (—)	7.37	7.79	7.48	7.55	0.19	2.56%	7.12	—
	$F_{D,target_2}$ (kN)	46.60	47.60	47.30	47.17	0.46	0.97%	46.17	48.17
	d_{target_2} (mm)	40.00	40.00	40.00	40.00	—	—	—	—
	μ (d_{target_2}) (—)	12.29	12.98	12.46	12.58	0.32	2.56%	11.87	—
	k_{el} (kN/mm)	8.78	9.57	8.77	9.04	0.41	4.57%	8.14	9.94
	k_{pl} (kN/mm)	0.49	0.49	0.52	0.50	0.02	3.12%	0.47	0.53
	Ductility class	H	H	H	—	—	—	—	—
Shear tests	$F_{D,y}$ (kN)	39.15	39.51	39.84	39.50	0.31	0.78%	38.83	40.17
	d_y (mm)	1.24	1.26	1.25	1.25	0.01	0.97%	1.23	1.28
	$F_{D,target}$ (kN)	40.71	38.87	39.12	39.57	0.89	2.25%	37.63	41.51
	d_{target} (mm)	24.00	24.00	24.00	—	—	—	—	—
	μ (d_{target}) (—)	19.39	18.98	19.13	19.17	0.19	0.97%	18.76	—
	$F_{D,peak}$ (kN)	43.91	43.49	44.45	43.95	0.43	0.98%	43.01	44.89
	d_{peak} (mm)	8.00	8.00	8.00	—	—	—	—	—
	μ (d_{peak}) (—)	6.46	6.33	6.38	6.39	0.06	0.97%	6.25	—
In bold the values used to compute γ_{Rd}									

Test	Parameter (units)	TEST 1	TEST 2	TEST 3	k^{mean}	SD	COV	EN 1990	
								k^-	k^+
	k_{el} (kN/mm)	31.64	31.25	31.75	31.55	0.23	0.74%	31.03	32.06
	k_{pl} (kN/mm)	0.00	0.00	0.00	—	—	—	—	—
	Ductility class	H	H	H	—	—	—	—	—
In bold the values used to compute γ_{Rd}									

Obtained results show that this bracket is characterized by a very high ductility resulting from a high elastic stiffness and displacement capacity. These properties confer to a CLT structure assembled with these connections a rigid behaviour with limited damage for low-intensity earthquakes, and a wide plastic range exploitable during strong seismic shocks. In particular, three displacement ranges can be identified to clarify the usage of the connector in high-ductility CLT buildings (Figs. 5, 6):

- *The elastic range* is characterized by high elastic stiffness and therefore high strength versus low displacement, which is favourable for static lateral loads (e.g., wind action) or low-intensity earthquakes (i.e., damage limitation state—DLS);
- *The working range* involves an optimal behaviour of the *X-bracket* in terms of high dissipative capacity and ductility, limited buckling phenomena, no pinching behaviour and low strength degradation: all conditions that are favourable for high-intensity earthquakes (i.e., ultimate limit state—ULS). The high stiffness in the elastic phase is clearly favourable also in this phase, to avoid excessive displacements before the required non-linearity is achieved (Smith et al. 2015);
- The high-ductility range is characterized by buckling phenomena during unloading, lower dissipative capacity and higher strength degradation than the working range. However, this range is useful to assure very high ductility, i.e., to avoid failure even if the working range is exceeded during the earthquake, guaranteeing a wider safety margin and redistribution of forces among connections, exploiting the redundancy of the building. This displacement range is not reached by traditional connections, which

normally fail for displacements lower than or equal to 30 mm (Gavric et al. 2015a).

3.2. Overstrength factor calculation

Results from tension tests of the *X-bracket* in Table 1 and Fig. 5b show that $d_{target_1} < d_{peak}$ and $d_{target_2} < d_{peak}$. According to the conceptual model presented in Sect. 2.1 and assuming $F_{D,code}^- = F_{D,y}^-$ (see Sect. 2.2) the overstrength factors γ_{Rd} and the sub-factors γ_{sc} and γ_{an} for the *X-bracket* loaded in tension can be computed according to Eqs. (2) to (4), considering $\gamma_{m,D}^- = \gamma_{m,D}^+ = 1.0$ and $\gamma_{cyc} = 1.0$. This last hypothesis can be accepted, considering the hysteretic behaviour of steel. Values for d_{target_1} and d_{target_2} are computed in Eqs. (7) and (8) respectively.

$$\gamma_{Rd} = \gamma_{sc} \cdot \gamma_{an} = \frac{F_{D,target_1}^+}{F_{D,target_1}^-} \cdot \frac{F_{D,target_1}^-}{F_{D,y}^-} = 1.07 \cdot 1.35 = 1.44 \quad 7$$

$$\gamma_{Rd} = \gamma_{sc} \cdot \gamma_{an} = \frac{F_{D,target_2}^+}{F_{D,target_2}^-} \cdot \frac{F_{D,target_2}^-}{F_{D,y}^-} = 1.04 \cdot 1.68 = 1.76 \quad 8$$

Results from the shear tests of the *X-bracket* in Table 1 and Fig. 6b show that $d_{target} > d_{peak}$ and $F_{D,target}^+ < F_{D,peak}^+$. According to the conceptual model presented in Sect. 2.1 and assuming $F_{D,code}^- = F_{D,y}^-$ (see Sect. 2.2) the overstrength factors γ_{Rd} and the sub-factors γ_{sc} and γ_{an} for the *X-bracket* loaded in shear can be computed according to Eqs. (2) to (4), again considering $\gamma_{m,D}^- = \gamma_{m,D}^+ = 1.0$ and $\gamma_{cyc} = 1.0$, Eq. (9).

$$\gamma_{Rd} = \gamma_{sc} \cdot \gamma_{an} = \frac{F_{D,peak}^+}{F_{D,peak}^-} \cdot \frac{F_{D,peak}^-}{F_{D,y}^-} = 1.04 \cdot 1.11 = 1.15 \quad 9$$

Table 2 shows a comparison in terms of γ_{Rd} among *X-bracket*, steel-to-timber joints with ring shank nails laterally loaded in parallel or perpendicular to face lamination of the CLT panel, screws to realize half-lap or LVL panel-to-panel joints and dowels. The values for nails, screws and dowels have been extrapolated from the literature (Gavric et al. 2015b; Izzi et al. 2016; Ottenhaus et al. 2017), assuming as $F_{D,code}^-$ the load-bearing capacities evaluated according to Eurocode 5 (CEN 2009), which are available in the same research works. It is worth noting that the obtained γ_{sc} for the *X-bracket* are lower than values for

traditional connections and close to 1.00 and that γ_{an} for the *X-bracket* in tension is mainly due to the hardening behaviour shown. Comparing the γ_{Rd} values between the *X-bracket* and the traditional connections it is evident the decrease of overstrength using a connection, which localizes the plastic deformation in a steel element, preserving the anchoring to the timber panel.

Table 2

Comparison of overstrength factors for the *X-bracket*, nails, screws and dowels

Connector/fastener	γ_{sc}	γ_{an}	γ_{Rd}
<i>X-bracket</i> in tension at d_{target_1}	1.07	1.35	1.44 ⁽¹⁾
<i>X-bracket</i> in tension at d_{target_2}	1.04	1.68	1.76 ⁽¹⁾
<i>X-bracket</i> in shear	1.04	1.11	1.15 ⁽¹⁾
Nails loaded parallel to face lamination ^a	1.27	1.61	2.04
Nails loaded perpendicular to face lamination ^a	1.53	1.69	2.59
Panel-to-panel joints with screws (half-lap joint) ^b	1.88	0.95	1.79 ⁽¹⁾
Panel-to-panel joints with screws (LVL joint) ^b	1.52	1.37	2.08 ⁽¹⁾
Dowels ^c	1.51 ⁽²⁾	1.29 ⁽²⁾	1.95
^a Values extrapolated from Izzi et al. (2016)			
^b Values extrapolated from Gavric et al. (2015b)			
^c Values extrapolated from Ottenhaus et al. (2017)			
⁽¹⁾ $\gamma_{cyc} = 1$ assumed			
⁽²⁾ Mean value of factors computed for the three layouts tested in monotonic loading			

4. Practical application of capacity design

A comparative application of capacity design to a traditional and an innovative connection, according to the conceptual model presented in Sect. 2.1, is here discussed. The *X-bracket* is considered for the application to an innovative connection. In this case, the brittle components are the fasteners to anchor the bracket to the CLT panel, which should assure small elastic deformations and therefore limited pinching phenomenon. An additional test of a specimen composed by the *X-brackets* fastened to a CLT panel, i.e., the complete connection, is also reported to evaluate the actual loss in strength and dissipative capacity, due to deformation of fasteners. With reference to traditional connections, the capacity design of a hold-down is proposed, to evaluate the

minimum design strength of the steel plate working in tension (brittle part of the system), depending on the number of ring shank nails (ductile part) in the hold-down.

4.1. Innovative connection

4.1.1. Design of the fastening to the CLT panel

The anchoring of the *X-bracket* to a CLT panel subjected to tensile loads was designed, referring to the mechanical properties of the bracket in tension and γ_{Rd} at $d_{target,2}$ evaluated in Sect. 3.2. The timber element is a 120 mm thick CLT panel composed by 5 layers of C24 timber boards. The two 16 mm diameter upper fixing points of the *X-bracket* are supposed to be fastened to the panel with two 16×200 mm 8.8-class calibrated bolts, to allow the horizontal arms to rotate and to dissipate energy due to steel plasticization. These two cylindrical restraints are subjected to high concentrated forces, which would result in predominant wood embedment, compromising the dissipative properties of the connection. Several techniques are available to improve both strength and stiffness of dowel-type joints and to reduce the pinching phenomenon (e.g., punched steel plates, toothed plate connectors, hollow steel tubes) (Rodd and Leijten 2003). In this application, a technique similar to punched metal plates (Blaß and Schmid 2000) has been chosen, using a thin steel plate placed between the bracket and the panel with two 16 mm diameter holes in correspondence to the fixing points of the bracket. A rectangular S275JR steel plate with dimensions of $330 \times 200 \times 3$ mm, was designed and fastened to the panel with fourteen 8×100 mm self-tapping partially threaded screws. The characteristic load-bearing capacity of the screws, $F_{B,code}^-$, was computed according to Eurocode 5 (CEN 2009). In detail, a total shear strength $F_{B,code}^- = 52.86$ kN was obtained for the effective number of screws, evaluating the characteristic embedment strength in timber member, $f_{h,k}$, according to Eurocode 5 formulation (CEN 2009), assuming the fastener yield moment $M_{y,Rk}$ and withdrawal capacity $f_{ax,k}$ according to ETA-11/0027 (ETA-Danmark 2016) and the characteristic value of panel density ρ_k equal to 385 kg/m^3 . This value of $F_{B,code}^-$ is higher than $\gamma_{Rd} \cdot F_{D,code}^- = 48.24$ kN (assuming again $F_{D,code}^- = F_{D,y}^-$), thus fulfilling Eq. (6) and complying with the capacity design.

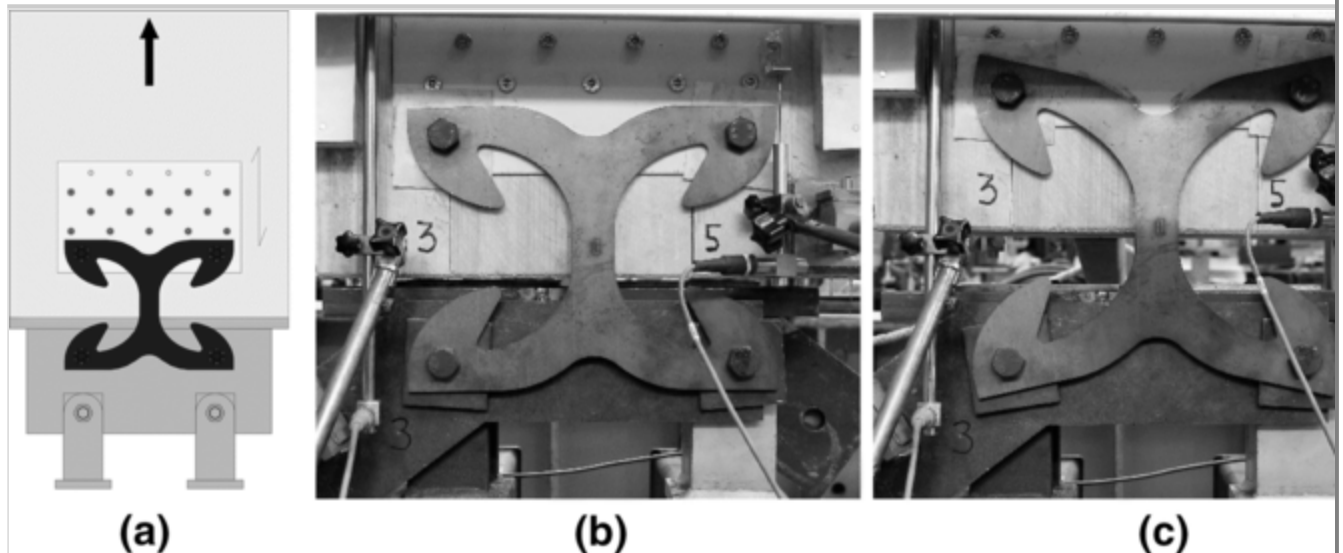
4.1.2. Experimental test of the bracket fastened to CLT

A cyclic-loading test of the complete connection was conducted, following the same cyclic-loading procedure and setup adopted for the bracket, in order to obtain a direct comparison between the hysteretic behaviour of the *X-bracket* and of the complete connection. The experimental test of the complete

connection was conducted only in tension. However, by changing the plate dimensions and the position of the screws, it is possible to realize the same over-resistant connection in case of shear loading conditions. Figure 7 shows the photos of the undeformed and deformed specimen.

Fig. 7

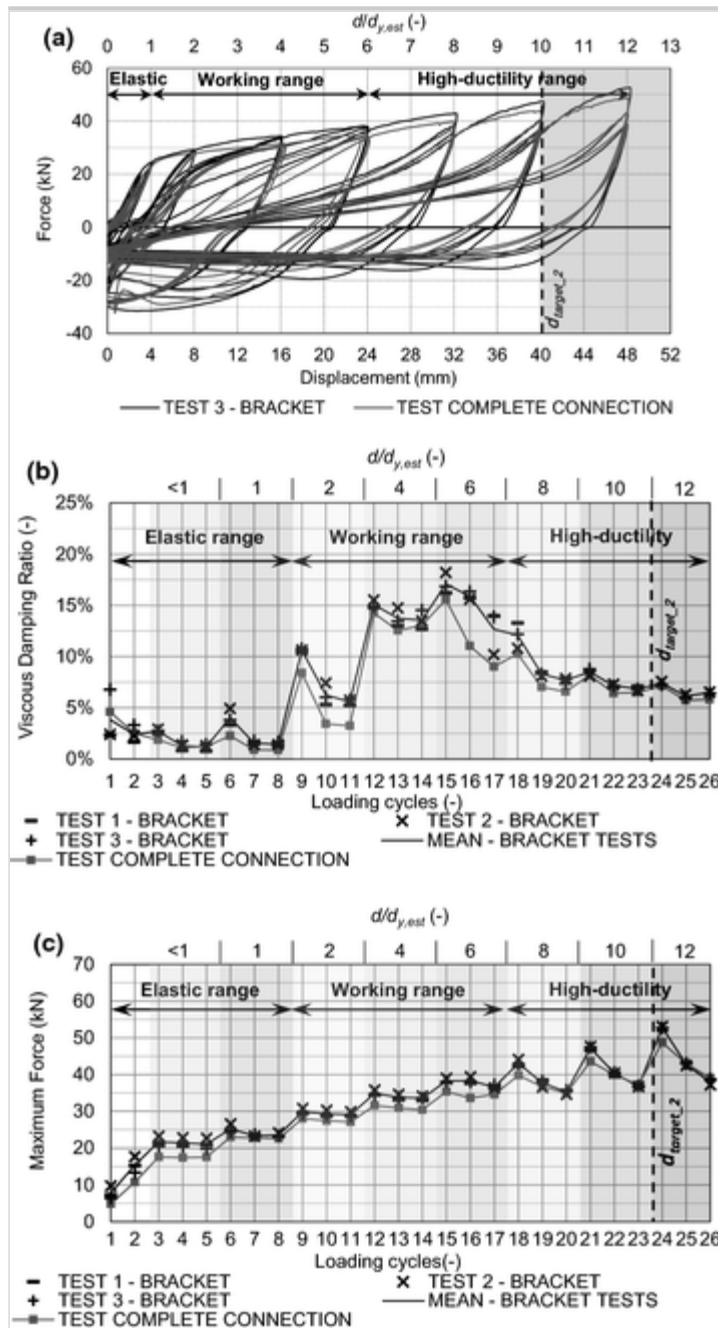
Test of the complete connection: **a** tested specimen; **b** photo of the undeformed specimen; **c** specimen at vertical displacement equal to 48 mm



From the superimposition of the results recorded for the *X-bracket* and the test of the complete connection, a very similar hysteresis behaviour (Fig. 8a) and a negligible decrease of dissipative capacity and strength were recorded (Fig. 8b, c).

Fig. 8

Comparison among tests of brackets and of the complete connection in tension: **a** hysteresis cycles; **b** equivalent viscous damping; **c** maximum force per loading cycle ($d_{y,est} = 4.0$ mm)



The reduction of strength and dissipative capacity [in terms of viscous damping ratio ν_{eq} (CEN 2005)] for the complete connection with respect to the mean value from the three tests of the *X-bracket* can be quantified from a comparison of the red and the black lines in Fig. 8b, c for all the loading cycles. It can be noted that no relevant strength reduction was recorded: a mean difference in strength equal to 2.75 kN (about 8.0%) was obtained in the working range and lower value in the high-ductility range. This proves that in the high-ductility range, characterized by the highest tensile loads, the proposed connection system is still able of withstanding the imposed loads and the hardening behaviour of the *X-bracket* (included in $\gamma_{Rd} = 1.76$) is completely exploited, in compliance with the capacity design approach. A slight decrease of viscous damping ratio was recorded in the working range. However, the resulting values show again the high dissipation capability of the *X-bracket* also considering the slight reduction

of performances due to the low elastic deformation of the fastening system. The recorded viscous damping ratios both in the working and in the high-ductility range are substantially higher than traditional hold-downs, which have ν_{eq} of about 3.0% due to marked pinching behaviour of nails (Gavric et al. 2015a).

4.2. Traditional hold-down

The minimum design strength $F_{B,code}^-$ of the steel plate of an hold-down working in tension with a certain number of nails is here evaluated according to Eq. (6). The main properties of the connection have been chosen to be consistent with specimens tested in Izzi et al. (2016), from which γ_{Rd} was taken: the timber element is a 5-layer 134 mm thick CLT panel; the ductile component is represented by 4×60 mm ring shank nails; the thickness of the steel plate is equal to 4 mm. Additional material properties and details are available in Izzi et al. (2016).

The hold-down to be designed is supposed to be fastened with 18 nails, hypothetically required to withstand the seismic force. The total load-bearing capacity of nails according to Izzi et al. (2016), using the analytical calculation model in Eurocode 5 (CEN 2009), is equal to $F_{D,code}^- = 18 \cdot 2.16 \text{ kN} = 38.9 \text{ kN}$. Therefore, the minimum load-bearing capacity of the steel plate to comply with Eq. (6) is $F_{B,code}^- \geq \gamma_{Rd} \cdot F_{D,code}^- = 2.04 \cdot 38.9 = 79.4 \text{ kN}$. The steel plate can be designed according to Eurocode 3 (CEN 2015), evaluating the minimum cross-section and steel class to comply with Eq. (10), where A and A_{net} are respectively the gross and net cross-section, f_y and f_u are the yielding and ultimate strength of structural steel.

$$F_{B,code}^- = \min (A \cdot f_y; 0.9 \cdot A_{net} \cdot f_u) \quad 10$$

Considering in the evaluation of the net cross-section of the steel plate three aligned 5 mm-diameter holes for fasteners, the resulting element could have a gross cross-section equal to 60×4 mm and a steel class S355, obtaining $F_{B,code}^- = 82.6 \text{ kN} > 79.4 \text{ kN}$, thus verifying the capacity design.

It is worth noting that the hold-down considered in this example does not correspond to a particular commercial hold-down but it was specifically designed to comply with capacity design. This does not limit the usage of commercial hold-downs, which normally have thickness of 3 mm, in particular when tests are available to certify the compliance with capacity design up to a predetermined target displacement. On the contrary, when the hold-down is not tested to verify the compliance with capacity design and the conceptual model is

not fulfilled, partial nailing is suggested in order to assure a ductile failure of the connection.

5. Conclusions

This work demonstrates that a key issue in the design of earthquake-resistant CLT structures is providing reliable overstrength factors to design the brittle components of a connection, in order to assure the exploitation of the plastic deformability of the ductile component. To this aim, a conceptual model has been presented as an enhancement of those available in the literature, to account for all the factors influencing the capacity design of a connection. The new concepts introduced are: the definition of a target displacement for the ductile component as limit of the displacement capacity according to the seismic performance demand; the application of the partial factor for material properties in the capacity design model both in the evaluation of the lower and upper design strength. These modifications are quite important, considering some specific issues of steel-to-timber connections as: the uncertainty in evaluating the actual load-bearing capacity of fasteners; the gap between the partial factor for material properties for steel structures and for connections for timber structures; the high ductility reached by innovative connections.

Data presented in the paper highlight that the use of innovative connections, which exploit the hysteretic behaviour of steel to confer to the structure a highly dissipative behaviour, can simplify and make more reliable the application of capacity design than the use of traditional connections, thanks to a well-defined behaviour of the ductile component and reliable response of structural steel. Analysed results demonstrate that the variability of the overstrength factor can be due not only to the statistical variability of the strength of the ductile element but also to the analytical method to estimate its characteristic strength, according to a particular code. It is fundamental therefore that the overstrength values proposed by a code be also consistent with the analytical method and parameters used to compute the load-bearing capacity of the elements considered to be ductile.

Original experimental results of an innovative connection named X-Bracket have been presented. The experimental characterization showed many advantages with respect to traditional connections: (1) higher ductility, displacement capacity and dissipative capacity; (2) very low scattering of results and well-defined yielding and failure conditions, resulting in a lower overstrength value and a more reliable application of capacity design; (3) negligible strength degradation and pinching behaviour in its working range.

Finally, the work summarized the reliable overstrength factors to be used by practitioners in the design of CLT structures assembled with traditional or innovative connection devices, specifying the quote due to statistical scattering and code overdesign.

Publisher's Note

Springer Nature remains neutral with regard to jurisdictional claims in published maps and institutional affiliations.

Acknowledgements

Economical support from “Proof of Concept Network” (PoCN) project, organized and managed by AREA Science Park (Trieste-Italy), financed by MIUR within “Progetti Premiali 2011” action, is acknowledged. Title of the specific project: “foundation system for timber and lightweight structures—ref. UNIPD_03”. Grateful thanks go to the staff of the Mechanical Testing Laboratory of Department ICEA of the University of Padova for their support during experimentation.

References

Baird A, Smith T, Palermo A, Pampanin S (2014) Experimental and numerical study of U-shape flexural plate (UFP) dissipators. In: 2014 NZSEE conference, pp 1–9

Blass HJ, Schmid M, Litze H, Wagner B (2000) Nail plate reinforced joints with dowel-type fasteners. In: 6th world conference on timber engineering (WCTE)

Ceccotti A (2008) New technologies for construction of medium-rise buildings in seismic regions: the XLAM case. *Struct Eng Int J Int Assoc Bridg Struct Eng* 18:156–165. <https://doi.org/10.2749/101686608784218680>

CEN (2004) EN 10025-2 hot rolled products of structural steels—technical delivery conditions for non-alloy structural steels. CEN, Brussels

CEN (2005) EN 12512. Timber structures—test methods—cyclic testing of joints made with mechanical fasteners. CEN, Brussels

CEN (2006) EN 14358 timber structures—calculation of characteristic 5-percentile values and acceptance criteria for a sample. CEN, Brussels

CEN (2009) EN 1995-1-1 Eurocode 5: design of timber structures—part 1-1: general—common rules and rules for buildings. CEN, Brussels

CEN (2010) EN 1990 Eurocode: basis of structural design. CEN, Brussels

CEN (2013) EN 1998-1 Eurocode 8: design of structures for earthquake resistance—part 1: general rules, seismic actions and rules for buildings. CEN, Brussels

CEN (2015) EN 1993-1-1 Eurocode 3: design of steel structures—part 1-1: general rules and rules for buildings. CEN, Brussels

ETA-Danmark (2016) ETA-11/0027 Screws for use in timber constructions

Flatscher G, Schickhofer G (2015) Shaking-table test of a cross-laminated timber structure. *Proc Inst Civ Eng Struct Build* 168:878–888.
<https://doi.org/10.1680/stbu.13.00086>

Foliente GC (1996) Issues in seismic performance testing and evaluation of timber structural systems. In: *Proceedings of the international wood engineering conference*, pp 29–36

Follesa M, Fragiaco M, Vassallo D et al (2015) A proposal for a new background document of chapter 8 of Eurocode 8. In: *International network on timber engineering research (INTER)*, Sibenik, pp 369–387

Follesa M, Fragiaco M, Casagrande D et al (2018) The new provisions for the seismic design of timber buildings in Europe. *Eng Struct* 168:736–747.
<https://doi.org/10.1016/j.engstruct.2018.04.090>

Foschi RO, Bonac T (1977) Load-slip characteristics for connections with common nails. *Wood Sci* 9:118–123

Frangiaco M, Dujic B, Sustersic I (2011) Elastic and ductile design of multi-storey crosslam massive wooden buildings under seismic actions. *Eng Struct* 33:3043–3053. <https://doi.org/10.1016/j.engstruct.2011.05.020>

Gavric I, Frangiaco M, Ceccotti A (2013) Capacity seismic design of X-LAM wall systems based on connection mechanical properties. In: *CIB-W18 meeting 46*, pp 287–298

Gavric I, Fragiaco M, Ceccotti A (2015a) Cyclic behaviour of typical metal connectors for cross-laminated (CLT) structures. *Mater Struct Constr* 48:1841–1857. <https://doi.org/10.1617/s11527-014-0278-7>

Gavric I, Fragiaco M, Ceccotti A (2015b) Cyclic behavior of typical screwed connections for cross-laminated (CLT) structures. *Eur J Wood Wood Prod* 73:179–191. <https://doi.org/10.1007/s00107-014-0877-6>

Hashemi A, Zarnani P, Masoudnia R, Quenneville P (2017) Seismic resistant rocking coupled walls with innovative resilient slip friction (RSF) joints. *J Constr Steel Res* 129:215–226. <https://doi.org/10.1016/j.jcsr.2016.11.016>

Henry RS, Aaleti S, Sritharan S, Ingham JM (2010) Concept and finite-element modeling of new steel shear connectors for self-centering wall systems. *J Eng Mech* 136:220–229. [https://doi.org/10.1061/\(ASCE\)EM.1943-7889.0000071](https://doi.org/10.1061/(ASCE)EM.1943-7889.0000071)

Izzi M, Flatscher G, Fragiaco M, Schickhofer G (2016) Experimental investigations and design provisions of steel-to-timber joints with annular-ringed shank nails for cross-laminated timber structures. *Constr Build Mater* 122:446–457. <https://doi.org/10.1016/j.conbuildmat.2016.06.072>

Izzi M, Casagrande D, Bezzi S et al (2018a) Seismic behaviour of cross-laminated timber structures: a state-of-the-art review. *Eng Struct* 170:42–52. <https://doi.org/10.1016/J.ENGSTRUCT.2018.05.060>

Izzi M, Polastri A, Fragiaco M (2018b) Investigating the hysteretic behavior of cross-laminated timber wall systems due to connections. *J Struct Eng* 144:04018035. [https://doi.org/10.1061/\(ASCE\)ST.1943-541X.0002022](https://doi.org/10.1061/(ASCE)ST.1943-541X.0002022)

Johansen KW (1949) Theory of timber connections. *Int Assoc Bridg Struct Eng* 9:249–262. <https://doi.org/10.5169/seals-9703>

Jorissen A, Fragiaco M (2011) General notes on ductility in timber structures. *Eng Struct* 33:2987–2997. <https://doi.org/10.1016/j.engstruct.2011.07.024>

Kelly JM, Skinner RI, Heine AJ (1972) Mechanism of energy absorption in special devices for use in earthquakes resistant structures. *Bull New Zeal Natl Soc Earthq Eng* 5:63–88

Latour M, Rizzano G (2015) Cyclic behavior and modeling of a dissipative connector for cross-laminated timber panel buildings. *J Earthq Eng* 19:137–171. <https://doi.org/10.1080/13632469.2014.948645>

Loo WY, Kun C, Quenneville P, Chouw N (2014) Experimental testing of a rocking timber shear wall with slip-friction connectors. *Earthq Eng Struct Dyn* 43:1621–1639. <https://doi.org/10.1002/eqe.2413>

Marchi L, Trutalli D, Scotta R et al (2016) A new dissipative connection for CLT buildings. In: *Proceedings of the 3rd international conference on structures and architecture ICSA 2016*. *Structures and Architecture* 17:169–177

Ottenhaus LM, Li M, Smith T, Quenneville P (2017) Overstrength of dowelled CLT connections under monotonic and cyclic loading. *Bull Earthq Eng*. <https://doi.org/10.1007/s10518-017-0221-8>

Paulay T, Priestley MJN (1992) *Seismic design of reinforced concrete and masonry buildings*

AQ2

Polastri A, Pozza L (2016) Proposal for a standardized design and modeling procedure of tall CLT buildings. *Int J Qual Res* 10:607–624. <https://doi.org/10.18421/IJQR10.03-12>

Polastri A, Giongo I, Piazza M (2017) An innovative connection system for cross-laminated timber structures. *Struct Eng Int* 27:502–511. <https://doi.org/10.2749/222137917X14881937844649>

Pozza L, Trutalli D (2017) An analytical formulation of q-factor for mid-rise CLT buildings based on parametric numerical analyses. *Bull Earthq Eng* 15:2015–2033. <https://doi.org/10.1007/s10518-016-0047-9>

Pozza L, Scotta R, Trutalli D et al (2016) Experimentally based q-factor estimation of cross-laminated timber walls. *Proc Inst Civ Eng Struct Build* 169:492–507. <https://doi.org/10.1680/jstbu.15.00009>

Ramberg W, Osgood WR (1943) Description of stress–strain curves by three parameters. *Natl Advis Comm Aeronaut*. Technical note no. 902. <https://doi.org/10.1016/j.matdes.2009.07.011>

Rodd PD, Leijten AJM (2003) High-performance dowel-type joints for timber structures. *Prog Struct Eng Mater* 5:77–89. <https://doi.org/10.1002/pse.144>

Schmidt T, Blaß HJ (2017) Dissipative joints for CLT shear walls. In: International network on timber engineering research (INTER)

Scotta R, Marchi L, Trutalli D, Pozza L (2016) A dissipative connector for CLT buildings: concept, design and testing. *Materials (Basel)* 9:9030139. <https://doi.org/10.3390/ma9030139>

Smith T, Moroder D, Sarti F et al (2015) The reality of seismic engineering in a modern timber world. In: International network on timber engineering research (INTER), Sibenik

Sustersic I, Fragiaco M, Dujic B (2012) Influence of the connection behaviour on the seismic resistance of multi-storey crosslam buildings. In: World Conference on Timber Engineering (WCTE)

Tomasi R, Smith I (2015) Experimental characterization of monotonic and cyclic loading responses of CLT panel-to-foundation angle bracket connections. *J Mater Civ Eng* 27:04014189. [https://doi.org/10.1061/\(ASCE\)MT.1943-5533.0001144](https://doi.org/10.1061/(ASCE)MT.1943-5533.0001144)